Depth of the vadose zone controls aquifer biogeochemical conditions and extent of anthropogenic nitrogen removal

Szymczycha B[1, 2*], Kroeger KD[2], Crusius J[3], Bratton JF[4]

[1]Institute of Oceanology Polish Academy of Sciences, Powstańców Warszawy 55, 81-712, Sopot, Poland

[2]USGS Woods Hole Coastal and Marine Science Center, 384 Woods Hole Road, Woods Hole, MA 02543, USA

[3]USGS at UW School of Oceanography; 1492 NE Boat St.; Box 355351; Seattle, WA 98195

[4]LimnoTech, 501 Avis Drive, Ann Arbor, MI 48108, USA

*corresponding author

Keywords:

Excess air, recharge temperature, MIMS, groundwater discharge, dissolved organic carbon, denitrification

Abstract

We investigated biogeochemical conditions and watershed features controlling the extent of nitrate removal through microbial dinitrogen (N_2) production within the surficial glacial aquifer located on the north and south shores of Long Island, NY, USA. The extent of N_2 production differs within portions of the aquifer, with greatest N_2 production observed at the south shore of Long Island where the vadose zone is thinnest, while limited N_2 production occurred under the thick vadose zones on the north shore. In areas with a shallow water table and thin vadose zone, low oxygen concentrations and sufficient DOC concentrations are conducive to N_2 production. Results support the hypothesis that in aquifers without a significant supply of

sediment-bound reducing potential, vadose zone thickness exerts an important control of the extent of N_2 production. Since quantification of excess N_2 relies on knowledge of equilibrium N_2 concentration at recharge, calculated based on temperature at recharge, we further identify several features, such as land use and cover, seasonality of recharge, and climate change that should be considered to refine estimation of recharge temperature, its deviation from mean annual air temperature, and resulting deviation from expected equilibrium gas concentrations.

1.1 Introduction

The rapid expansion of suburban populations along the coast has significant impact on aquifer resources by both increasing the demands for potable water and by increasing nitrogen additions to groundwater through atmospheric deposition, fertilizer applications, sewage disposal and general infiltration/recharge. Consequently, increased nitrogen loads via groundwater discharge can enhance primary production in coastal seas (Paerl, 1997) and cause eutrophication (Valiela et al., 1978; Johannes, 1980; Capone and Bautista, 1985, Lee et al., 2009).

The human population density has increased over the last several decades on Long Island, NY, USA leading to both greater nitrogen inputs to the landscape (Flipse et al., 1984; Young et al., 2013), and increased nitrate concentration in groundwater (Abdene et al., 2010; Böhlke et al., 2009; Young et al., 2013). In some areas located on the north shore of Long Island the groundwater nitrate concentration exceeds the federal drinking water limit of 714 μM (Young et al., 2013). Hence, understanding processes related to transport and attenuation of nitrate in aquifers can improve management of groundwater as a drinking water reservoir and as a vector for nutrient inputs to the coastal marine environment.

Fixed nitrogen may be added to the environment in reduced forms, including organic N and ammonium, or in oxidized forms, dominated by nitrate. NO_3^- is typically the dominant form of dissolved inorganic nitrogen (DIN) in oxic aquifers, moving freely through the unsaturated and

saturated zone while ammonium (NH_4^+) tends to dominate the DIN pool in suboxic aquifers, however its transport is slower due to chemical sorption and exchange with aquifer sediments (Böhlke et al., 2006). NO_3^- is a highly mobile form of nitrogen in soil and aquifers, and in many cases is the primary form transported to aquifers. The fate of NO_3^- after crossing the water table and leaving contact with unsaturated soil is determined by varying biogeochemical conditions along flow paths through the aquifers (Korom, 1992) and may be determined by any of several processes including dissimilatory nitrate reduction to ammonium (DNRA), assimilation of nitrate into microbial biomass (Hill, 1996), nitrate removal via phreatophytes (Schnoor et al., 1995) and reduction to N_2 gas. Denitrification and anaerobic ammonium oxidation (anammox) remove NO_3^- as gaseous products. Denitrification reduces NO_3^- via nitrite (NO_2^-), nitric oxide (NO) and nitrous oxide (N_2O) to the non-reactive dinitrogen gas (N_{2DEN}) while anammox uses NO_2^- or NO_3^- as an electron acceptor in the oxidation of NH_4, to yield N_2. In contrast, DNRA retains N within the ecosystem by recycling NO_3^- into NH_4^+. Denitrification has generally been considered to be the most significant fixed nitrogen removal process in aquifers, while mechanisms such as anammox, DNRA and assimilation of nitrate into microbial biomass are likely to be secondary (Rivett et al., 2008; Böhlke et al., 2009; Young et al., 2013). A recent study, however, suggested that the rate of N_2 production through anammox may be similar to the rate of denitrification, under certain conditions that may be common within aquifers (Smith et al. 2015). In general, anammox has increasing importance relative to denitrification where the ratio of nitrate to dissolved organic carbon (DOC) is greater (Babbin et al., 2013; Algar et al., 2014; Kraft et al., 2014). As we will show in the current study, under those conditions, at two of our study sites, the rate of N_2 production is relatively low, while increasing DOC concentrations at a third site lead to a substantially greater rate of N_2 production. Thus, we interpret heterotrophic denitrification to be

the primary driver of N_2 production in the present study, while acknowledging that anammox likely plays an unquantified role as well.

Denitrification is controlled by environmental conditions, and generally requires co-occurrence of nitrate, denitrifying bacteria, an electron donor (primarily organic carbon, reduced iron, or reduced sulfur), and low oxygen conditions (Seitzinger et al., 2006). Temperature, pH, and availability of other nutrients are also suggested to exert secondary influence on denitrification rates (Rivett et al., 2008).

Although the biogeochemical conditions controlling denitrification are reasonably well-understood, controls on occurrence in aquifers are poorly known. Variations in DOC concentration in a glacial, sand and gravel aquifer were suggested to depend on vadose zone thickness by Pabich et al.(2001). Similarly, dissolved organic nitrogen (DON) concentrations, and the proportion of total dissolved N as DON, are negatively correlated with vadose zone thickness (Kroeger et al. 2006). Both hypotheses assume that microbial remineralization, and to a lesser degree adsorption, in the mineral soil transforms DOC to CO_2 and transforms DON primarily to nitrate. Young et al. (2013) proposed a refinement on the mechanism by which a thick vadose zone can promote oxygenation of recharging groundwater, and therefore increased oxidative biogeochemical processes in the vadose zone and aquifer. The mechanism involves compression and expansion of the air column that occupies the pore spaces in the unsaturated zone, due to variations in barometric pressure, with the predicted depth of pore space ventilation increasing exponentially with increasing vadose zone thickness. The presented findings suggest that unsaturated zone thickness can have a strong influence on biogeochemical conditions in aquifers, and thus may influence the extent of denitrification. Hence, the aim of this study was to measure denitrification in aquifers recharged through varying vadose zones, under otherwise similar hydrogeological conditions, and thus test whether the vadose zone thickness determines

biogeochemical conditions that control nitrate attenuation in the aquifer. We used membrane inlet mass spectrometry (MIMS), which enables the direct measurement of dissolved gases, including N_2 and Ar. Calculating excess N_2concentrations due to denitrification relies critically on knowledge of the temperature at which groundwater recharged to the aquifer. Commonly in studies of noble gases in aquifers, recharge temperature is assumed to be approximately equal to the long-term mean annual air temperature (Stute et al., 1995). In this study, results indicated recharge occurred at temperatures substantially greater than mean annual air temperature. We present several features that should be considered to refine estimation of recharge temperature and its deviation from mean annual air temperature, in the context of a range of vadose zone thickness, seasonality of recharge, climate change, groundwater age, and land use and cover.

2.1 Materials and Methods

2.1.1 Study Sites

Long Island's aquifers consist of a wedge of unconsolidated Cretaceous sands, gravels, silts and clay overlain by glacial sediments (Monti and Scorca, 2003). Precipitation is the source of freshwater recharge to the aquifer system (Swarzenski, 1963; Lusczynski and Swarzenski, 1966; Peterson, 1987, Steeinhuis et al., 1985; Monti and Scorca, 2003). There is a groundwater divide running east-west along the axis of the island, and flow of water is dominantly to the north or to the south from that divide. The southern part of the island is a gently sloping outwash plain, while the north shore consists of an eroded moraine with steep slopes and narrow beaches. The north part of Long Island (LI) is characterized by a deeper water table and a thicker layer of unsaturated soil (vadose zone) than the south shore (Monti and Busciolano, 2009).

This study was designed to include sites on both north and south shores in order to represent the different geological settings (Cross et al., 2012; Cross et al., 2013). The three sites were located near the towns of Manhasset (Manhasset Bay -MB), Northport (Northport Harbor-

NH), and Patchogue (Great South Bay-GSB) (Fig. 1). MB is located near the western end of Long Island, on the shore of Long Island Sound, approximately 25 km east of Manhattan. NH is a portion of Northport Bay, located ~32 km east of the MB site. Patchogue is on the south shore of eastern Long Island, ~32 km southeast of the NH site. The human population density in the sampled portion of the Patchogue watershed (2,211/km^2) is approximately equal to that of Manhasset (2,523/km^2) while the density of Northport is somewhat lower (1074/km^2). Nitrogen is delivered to Long Island's groundwater mainly from atmospheric deposition, fertilizer applications, and wastewater disposal (Abbene et al., 2010; Zhao et al., 2011; Young et al., 2015). The study sites were selected to represent both sewered (Manhasset) and unsewered (Northport and Patchogue) watersheds, though we note that portions of the Patchogue area have since been sewered.

2.1.2 Sampling, laboratory analyses and statistical methods

Groundwater samples (n=79; salinity<0.8) were collected in spring and fall of 2008 (MB and NH) and fall of 2008 (GSB) along the shorelines, near or within the intertidal zone and at depths of 0.3–9.5m below the groundwater surface. Sample collection locations and depths below land surface were selected to provide samples of groundwater near the terminal end of groundwater flow-path from land to sea, and prior to mixing with saline groundwater. Such samples provide the best representation of chemical conditions and loads carried by terrestrial groundwater. Peristaltic pumps were used to collect groundwater samples from AMS (Piezometer Groundwater Sampling Kit) drive point samplers. Oxidation/reduction potential (ORP), pH, dissolved oxygen (DO) and salinity were measured in the field using multi-probe meters (YSI Pro Plus) with flow through cell. ORP readings were converted to Eh (mV) units by adding 200 to the values (Kroeger et al., 2007). Samples collected for other parameters were analyzed within two to four weeks.

Samples for dissolved organic carbon (DOC) were filtered (polyethersulfone cartridge filters, 0.45μm pore size), collected in acid rinsed, combusted glass bottles and acidified with HCl to a pH of 2 upon collection. Samples for nitrate (NO_3^-), nitrite (NO_2^-) and ammonium (NH_4^+) were filtered through the same filters and frozen. $NO_3^- + NO_2^-$ and NH_4^+ were analyzed by means of automated analyzer (Lachat Instruments FIA-6000) using standard colorimetric methods. Nitrate and nitrite were not quantified separately, and in this paper, their sum is referred to as ‘‘nitrate.’’ DOC was analyzed by persulfate digestion and nondispersive infrared detection method. The average relative standard deviation of three replicate injections of an intermediate standard was typically ±5%.

Samples for MIMS analysis of dissolved N_2 and Ar were collected with no headspace in 12-ml glass vials with screw cap butyl rubber septa. Vials were filled from the bottom, overflowed with >5 void volumes, and stored under water at <4°C. Generally, in MIMS analysis the liquid sample is pumped past a gas-permeable, silicone membrane for degassing. The gasses then pass through a liquid nitrogen trap to remove water vapor and CO_2 and through a copper reduction tube maintained at 600°C to remove oxygen. Oxygen removal is necessary to avoid formation of NO in the ion source. Mass measurements were made on a quadrupole mass spectrometer (Balzers Prisma). The instrument response was measured for masses 28, 29, 30 and 40; the three masses of N_2 and the main Ar mass. The MIMS responds linearly to gas concentration, and a single point calibration was used for each mass. The primary standard for MIMS analyses is air-equilibrated water. This standard is prepared by allowing a constant-temperature, continuously-circulated bath of laboratory-grade water, with headspace at 100% relative humidity, to remain equilibrated with atmosphere and repeatedly sampled throughout the period of sample analyses. Instrument response is linear to a wide range of gas concentrations, and thus the single calibration standard is sufficient to achieve the accuracies reported. N_2 and Ar

/

measurements by MIMS have a precision of <0.5 % (Kana et al., 1994). Occasionally samples can lose gas during samples collection, and data from such degassed samples were not used in interpretation of study results..

The age, or time since recharge, of groundwater samples (n=7) collected during this study was estimated based on mass spectrometric measurement of helium isotopes and tritium analysis of water samples. Sample analysis and age estimation were conducted by the Lamont-Doherty Earth Observatory, using the ^{3}He ingrowth method. Precisions for measurement of tritium, $\delta^{3}He$, and the ^{4}He and Ne concentrations are ±1 to 2%, ±0.15 to 0.2%, and ±0.2 to 0.3%, respectively, and reported age uncertainty for the samples analyzed ranged from 0.1 yr to 1.2 yr.

The vadose zone thickness for each watershed was calculated by first delineating areas contributing discharge to sampled portions of shoreline on the basis of water table elevation contours, with flow lines perpendicular to the contours. Watershed boundaries were then overlaid onto a map of modeled vadose zone thickness on Long Island (Monti and Busciolano, 2009) using GIS software, and average vadose zone thickness was calculated for each contributing area. To verify whether the path length that recharging groundwater and dissolved constituents traverse through the vadose zone influences the biogeochemical conditions that control denitrification in the aquifer we used ANOVA and Kruskal-Wallis (KW-H) tests (STATISTICA software). Both statistical methods assess the significant differences on a continuous dependent variables by a categorical independent variables (with two or more groups). We grouped the groundwater samples from each site according to the watershed sections from which they were collected, and plotted the summary statistics of the biogeochemical parameters vs. the average vadose zone thickness in each watershed section (Fig. 4).

2.1.3 Determining R_{Temp}, calculating N_{2DEN}, excess air, $NO_3^-{}_{initial}$

Plots of N_2/Ar indicated that groundwater recharged at a range of temperatures that differed among three watersheds. Recharge temperature (R_{Temp}) was estimated separately for each site, based on several factors such as the minimum and maximum temperatures sufficient to explain measured Ar concentrations; records of air temperature at multiple nearby weather stations (NOAA, 2016) and seasonality of recharge. Differences in apparent recharge temperature among the sites suggested that a thin vadose zone can result in significant deviation of recharge temperature relative to mean annual air temperature, as will be discussed in the Results and Discussion section.

Sources for dissolved N_2 in groundwater are: 1) equilibration with the atmosphere and soil gas, with solubility determined by the temperature, salinity and pressure at the time that recharging water leaves the vadose zone and is no longer in contact with the atmosphere, 2) "excess air" resulting from dissolution of air bubbles that were entrapped during recharge, and 3) production by denitrification (Böhlke et al., 2002). Ar occurs in groundwater due to processes 1 and 2, and therefore can serve as a tracer to quantify N_2 from those sources. Hence, the dissolved gas sample concentration can be given as N_2/Ar ratios (Böhlke et al., 2002) corresponding to:

$$[N_{2Sample}]/[Ar_{Sample}]=([N_{2ASW}]+[N_{2EA}]+[N_{2DEN}])/([Ar_{ASW}]+[Ar_{EA}]) \quad (1)$$

where N_{2ASW} and Ar_{ASW} are the molar concentrations of nitrogen and argon due to equilibrium with the atmosphere at a given temperature, salinity and pressure. N_{2DEN} is the nitrogen gas product of the denitrification process. N_{2EA} and Ar_{EA} correspond to concentrations of nitrogen and argon coming from excess air. Excess air might occur due to complete or partial dissolution of bubbles (Holocher et al., 2002). If excess air results from complete dissolution, then the excess air component is identical to atmospheric air and can be calculated using the following equation (Böhlke et al., 2002):

$$[N_{2EA}]=([Ar_{sample}]-[Ar_{ASW}])*[N_{2AMF}]/[Ar_{AMF}] \quad (2)$$

where N_{2AMF} and Ar_{AMF} are atmospheric mole fractions of N_2 and Ar, respectively. The theoretical maximum degree of fractionation, or deviation from atmospheric mole fractions, can be calculated based on the ratio of equilibrium concentrations of N_2 and Ar at the temperature of recharge (Weymann et al., 2008; Young et al., 2013). In the present study, and in our experience in general with sampling surficial aquifers, the assumption of substantial fractionation would result in calculation of too high recharge temperatures and concentrations of excess air. Instead, results suggest that fractionation is minimal and our best approximation is an assumption of complete dissolution of bubbles, without fractionation.

The nitrate concentration prior to denitrification ($NO_3^-{}_{initial}$) was estimated for each sample by combining the measured values for NO_3^- and N_{2DEN} (Böhlke et al., 2002):

$$[NO_3^-{}_{initial}]=(2*[N_{2DEN}])+[NO_3^-] \quad (3)$$

For samples in which denitrification was not detected, the $NO_3^-{}_{initial}$ was assumed to equal measured NO_3^-. $NO_3^-{}_{initial}$ calculation was based on the assumption that denitrification is the main process responsible for nitrogen transformations on Long Island, NY, USA (Young et al., 2016) and other processes such as (dissimilatory nitrate reduction to ammonium) DNRA, nitrification, remineralization, and anammox (Smith et al., 2015) were not considered.

3.1 Results and discussion

3.1.1 Determination of R_{Temp}

Estimation of the recharge temperature is critical, since microbially-produced N_2 is calculated based on the measured concentration of N_2, in excess of the sum of atmospheric equilibrium and excess air due to dissolution of bubbles entrained during recharge. Dissolved argon concentration can be used to estimate recharge temperature and excess air, since measured concentrations (Ar_{Sample}) are equal to the sum of the molar concentrations due to equilibrium with atmosphere (Ar_{ASW}) and from excess air (Ar_{EA}):

$$[Ar_{Sample}]=[Ar_{ASW}]+[Ar_{EA}] \quad (4)$$

As has been noted, commonly equilibrium concentrations are calculated based on long-term, mean annual air temperature, and on Long Island, the mean annual air temperature (Tm) of 10.4°C (Bridgehampton), during the period from 1960 to 1990, has been used as in past studies of dissolved gases in aquifers (Böhlke et al., 2009; Young et al., 2013). In our study, Ar_{Sample} was variable, and was often lower than calculated argon concentration, Ar_{ASW}, due to equilibrium with the atmosphere at 10.4°C. Our interpretation is that recharge temperatures varied within sites and among sites, and were considerably warmer than Tm. Thus, we estimated a range of recharge temperatures for each site, based on the calculated (R_{Temp}) corresponding to the minimum and maximum Ar concentration, with support from interpretation of long term air temperature data across several decades, at several stations on Long Island (NOAA, 2006). Figure 2 presents an air-saturated water (ASW) curve plotted on each graph for a range of recharge temperatures, along with curves showing expected increase in gas concentrations with increasing amounts of excess air. Denitrification increases the concentration of N_2, without affecting Ar concentration, and thus shifts points to the right along the x-axis. As shown in Figure 2, recharge temperature was estimated at 12.2˚C to 13.0˚C in the GSB watershed, 11.8˚C to 12.6˚C at MB, and 10.4˚C to 11.8˚C at NH.

There are several features and processes that can be expected to cause variations inrecharge temperature and deviation from Tm. According to the IPCC, global air temperature at the land-surface has increased at a rate of approximately 0.13ºC per decade from 1950 to 2000 (IPCC, 2013), with even higher rates during the last few decades. A similar trend of Tm increase in the context of climate change is observed on Long Island. Tm showed an increasing trend during the period from 1930 to 2010 in Bridgehampton, LI, NY, USA (Fig. S1), with substantial change during the likely timeframe of recharge of water sampled in present study. The tracer-

based estimates of groundwater age, or time since recharge, in the analyzed samples was in the range of 0.4 yr to 16.0 yr (Table S1). Therefore, as a starting point, mean temperature during the 10-year and 20-year periods prior to sample collections were used to calculate Tm at each of the temperature monitoring stations during the calculated period of recharge (Fig. S2). Warming on the timescale of decades is evident from the consistently warmer mean air temperatures in the most recent decade, as compared to the most recent two decades.

The second consideration that is likely to influence effective recharge temperature is seasonal variability in the rate of recharge. In the study area there is a tendency toward a greater rate of recharge in the cooler seasons, due to a lower rate of evapotranspiration. Steenhuis et al. (1985) estimated that 75% of recharge on Long Island occurs between October and May, and accordingly recharge-weighted mean annual air temperatures for each weather station were calculated from monthly temperature averages.

Third, we note that there are important geographical variations in air temperatures, likely related to weather patterns, proximity to the coast, and to land use. With the highly-urbanized boroughs of New York City lying to the west, and generally upwind, of the study sites, and significant local variations in population density on Long Island itself, it can be expected that the heat island effect (U.S. EPA, 2014), could possibly cause both spatial variations, and a general increase in temperature. Temperatures recorded at stations located in the northwest portion of Long Island (e.g. the Mineola and Sea Cliff stations, near the MB watershed and only 13 km east of the borough of Queens; Fig.S2) had generally higher temperatures than stations located farther east (e.g. the Huntington and Centerport stations, in the NH watershed and 43 km east of the Bronx borough; the Patchogue, Mastic and Islip stations near the GSB watershed and 65 km west of Queens; Fig.S2). At the MB and NH study sites, the minimum and maximum R_{Temp} calculated based on argon concentrations are within the range of annual air temperatures measured at the

nearby temperature monitoring stations during the 10-year and 20-year time frames. R_{Temp} in the GSB watershed, based on dissolved gas concentrations, appears to have been higher than measured Tm at the nearby south shore stations (e.g. Patchogue, Islip, Mastic). Here, we offer a hypothesis that co-occurrence of urbanization and a thin vadose zone may explain the relatively warm recharge temperature. In densely-populated areas, with little tree cover and large impervious surface area, the opportunity for absorption of solar energy by soils is greater, due to the absence of both shade and the insulating layer of organic material common on the land surface in wooded areas. In a study located near GSB in the Babylon-Islip area on Long Island, NY, R_{Temp} in wooded areas was similar to Tm (approximately 10.5˚C during 1940-1960), while in residential areas R_{Temp} was found to be 0.6˚C to 2.2˚C higher (Pluhowski and Kantrowitz, 1964). The Babylon-Islip area has a thin vadose zone, similar to the average 2.3 m vadose zone in the GSB watershed (Fig. 4; Monti and Busciolano, 2009). Thus, where there is reduced tree cover and little separation between the warmed land surface and the depth of recharge to the water table, we should expect recharge to occur at temperatures that are often greater than prevailing air temperature. Conversely, where the vadose zone is thicker, such as at MB and NH (Fig. 4), soil and water temperature should approach Tm or wTm prior to recharge, as was observed in the present study. Hence, the temperature of recharge to shallow aquifers can be more readily influenced by factors at the land surface. We recommend to refine the estimation of recharge including the temporal variability of the mean air temperature, the age of the groundwater, the seasonality of recharge, land use and cover, and the thickness of the vadose zone.

3.1.2 Factors influencing the extent of denitrification

All samples were collected within or near the intertidal zone at depths of less than 10m, had salinity below 0.8 and were slightly acidic. Figure 3 shows a treatment of the gas data in which equilibrium concentrations at the estimated recharge temperature have been subtracted

from measured N_2 and Ar concentration. Thus, the plotted gas concentrations are attributed only to excess N_2 and Ar from dissolution of gas bubbles (excess air), and to the sum of N_{2EA} and N_{2DEN}. Arrows represent the direction of shift in N_2 concentration due to denitrification. The plots highlight the stark contrast among the sites in terms of extent of denitrification. The greatest amount of denitrification was observed in GSB, while in NH and MB limited denitrification was observed (Fig.3 and Table 1). In GSB denitrification (N_{2DEN}) was in the range of 18.7μM to 260.6μM and 85% of samples had N_{2DEN} higher than 100μM, indicating that 200μM of nitrate was reduced in 85% of samples. In MB N_{2DEN} ranged from 11.0 μM to 108.7μM while in NH N_{2DEN} ranged from 1.3μM to 103.3μM. Denitrification rates were generally three times higher in GSB than in MB and NH. The average and median N_{2DEN} for the sites equaled 142.6μM and 158.2 μM for GSB; 48.6 μM and 44.3 μM for MB; and 21.4 μM and 16.2 μM for NH. The biogeochemical conditions in aquifers are presented as the summaries of Eh, DO, DOC, NO_3, $NO_3^-{}_{initial}$, NH_4, N_2, Ar and N_{2DEN} in Table 1 while depth, salinity, pH, Eh , DO, DOC, NH_4, NO_3, N_2, Ar and N_{2DEN} for every sample are available in Table S2. Generally, NO_3 concentrations were high in both NH and MB and substantially lower in GSB. Both ANOVA and Kruskal–Wallis (KW-H) tests illustrated that NO_3 mean concentration from GSB significantly differs from means from both NH and MB (Table 1 and Fig.S3.). Two of the sites in the present study, NH and GSB, were not sewered while MB was sewered (Abbene, 2010; Zhao et al. 2011). Therefore, it could be assumed that the aquifer at NH and GSB receives more wastewater nitrogen loading, per capita, than MB. Population density, on the other hand, was roughly a factor of 2 greater in the MB and GSB watersheds than in NH, and thus nitrogen loading from fertilizer= can be expected to be greater where population density is greater. However, average $NO_3^-{}_{initial}$ were similar (Table 1, Fig.S3) and suggest a similar level of nitrogen loading at each of the sites. Both ANOVA and KW-H tests indicated that differences in $NO_{3initial}$ among sites are not significant ($p>0.005$).

Therefore, differences in nitrogen supply do not appear to explain the differences in extent of denitrification between sites. Other parameters controlling rates of denitrification such as Eh, DO, DOC significantly differed among sites ($p<0.005$). Eh values were generally high in samples collected in both NH and MB while GSB was characterized by reducing conditions. DO differed in GSB in comparison to both NH and MB. DOC concentrations were also found high in the GSB aquifer in comparison to NH and MB (Table1). High levels of denitrification (N_{2DEN}>100μM) generally occurred where DO was lower than 100μM, ORP lower than 200mV and DOC higher than 250μM (TableS2 and Fig.S4). Those results are consistent with the general understanding of the controls on denitrification in aquifers, indicating that the process should be favored where nitrate co-occurs with an electron donor, commonly organic carbon, and where the supply of oxygen is limited (synthesized by Rivett et al. 2008). Generally, at the NH and MB sites, low DOC concentrations, high DO concentrations and oxidizing conditions appear to limit the extent of denitrification, while at the GSB site, greater DOC availability and more reducing conditions promote greater denitrification. ANOVA showed that means of $N_{2DEN,}$ Eh, DO, DOC from GSB significantly differ from means from both NH and MB but separate groups of normality histograms were visible on the Gaussian curves (t-test). Therefore, it suggests that there is a factor controlling distribution of Eh, DO and DOC. To test whether the path length that recharging groundwater and dissolved constituents traverse through the vadose zone influences the biogeochemical conditions that control denitrification in the aquifer we used ANOVA and KW-H tests (Fig.4). The groundwater samples from each site were grouped according to the watershed sections from which they were collected, and plotted the summary statistics of the biogeochemical parameters vs. the average vadose zone thickness in each watershed section (Fig. 4). At the GSB site, the mean vadose zone thickness was estimated to be 2.3mand 32 groundwater samples were collected . NH received groundwater from three sampled watershed

sections and calculated mean vadose zone thicknesses were 32.7m (*n*=3), 41.5m (*n*=25) and 45.3m (n=9), while MB received water from two sampled watershed sections with the mean vadose zone thicknesses of 11.9m (n=4) and 21.9m (n=5). KW-H test showed that the means of Eh, DO, DOC and N_{2DEN} from GSB are significantly different from means of NH and MB. Consequently, where the vadose zones are thin, DOC concentrations are high, conditions are reducing, and extent of denitrification is greatest (Fig. 4). As vadose zones become thicker, conditions in the aquifer become more oxidizing, and DOC concentration and denitrification decrease dramatically. Pabich et al. (2001) showed that in a glacial outwash setting, DOC concentrations in groundwater decreased with increasing unsaturated zone thickness in the recharge area, and that concentrations decreased exponentially with increasing depth below the water table. With vadose zones thinner than 1.25 m, DOC concentrations were higher than 16,667 μM, while for vadose zone thicker than 5.0 m, DOC did not exceed 167 μM. Kroeger et al. (2006) investigated dissolved organic nitrogen (DON) in a series of watersheds with unconsolidated glacial aquifer sediments and found a negative correlation between unsaturated zone thickness and percent of total dissolved nitrogen (TDN) as DON. It was hypothesized that the preponderance of organic matter (DOC and DON) carried by recharging groundwater is removed from solution during transport through thick unsaturated zones, due primarily to oxidation to CO_2 and to nitrate and secondarily due to adsorption of organic matter (Pabich et al. 2001, Kroeger et al. 2006). Young et al. (2013) proposed a refinement on the mechanism by which a thick vadose zone can promote oxygenation of recharging groundwater, and therefore increased oxidative biogeochemical processes in the vadose zone and aquifer. The mechanism involves compression and expansion, due to passing weather fronts, of the air column that occupies the pore spaces in the unsaturated zone. The depth of pore space ventilation and oxygen renewal is much greater in areas with thicker vadose zones. Young et al. (2013) calculated that in

Northport, Long Island, NY with a vadose zone >10 m thick, advective air exchange due to typical variations in barometric pressure could replace 50% of the air column to a depth of 2 m below land surface. Therefore, a thick vadose zone was suggested to explain aquifer biogeochemical conditions including low dissolved organic carbon, high dissolved oxygen concentration, and minimal occurrence of denitrification.

4.1 Conclusions

The results presented here are consistent with the hypothesis that where the vadose zone is thin, DOC, sourced from the organic soil horizon and from root exudates (Rivett et al. 2008), is able to enter the aquifer with recharging groundwater. Here we further extend the evidence for this set of hypotheses related to vadose zone control of biogeochemical conditions in aquifers, and show for the first time that dissolved oxygen concentration, oxidation/reduction potential and extent of denitrification are also related to watershed vadose zone thickness.

5.1 Acknowledgments

Project supported by the Polish-U.S. Fulbright Commission, the USGS Coastal and Marine Geology Program, the National Fish and Wildlife Foundation, and the USGS/National Park Service Water-Quality Assessment and Monitoring program. We thank A. Mann, S. Brosnahan, M. Casso, W. Brooks, and L. Erban for technical support; S. Zhao and P.Zhang for participation in field collections; J. Monti, I. Abbene, C. Schubert and H. Bokuniewicz for discussions and information on Long Island sites. We are grateful to A. Giblin and J. Tucker of the MBL for access to and training on their MIMS. Any use of trade, firm, or product names is for descriptive purposes only and does not imply endorsement by the U.S. Government.

Literature

Abbene, I. J., 2010. Shallow groundwater Quality in the Village of Patchogue, Suffolk County, New York. U.S. Geological Survey, Scientific Investigations Report 2010–5132, 30pp.

Algar, C. K., Vallino, J. J., 2014. Predicting microbial nitrate reduction pathways in coastal sediments. Aquat. Microb. Ecol. 71, 223−238.

Babbin, A. R., Ward, B. B., 2013. Controls on nitrogen loss processes in Chesapeake Bay sediments. Environ. Sci. Technol. 47, 4189− 4196.

Böhlke, J.K., Wanty, R., Tuttle, M., Delin, G., Landon, M., 2002. Denitrification in the recharge area and discharge area of a transient agricultural nitrate plume in a glacial outwash sand aquifer, Minnesota. Water Resour. Res. 38, 10.1–10.26.

Böhlke, J. K., Smith, R. L., Miller, D. N., 2006. Ammonium transport and reaction in contaminated groundwater: Application of isotope tracers and isotope fractionation studies. Water Resour. Res. 42, W05411.

Böhlke, J.K., Hatzinger, P.B., Sturchio, N.C., Gu, B.H., Abbene, I., Mroczkowski, S.J, 2009. Atacama perchlorate as an agricultural contaminant in groundwater: isotopic and chronologic evidence from Long Island, New York. Environ Sci Technol 43, 5619–5625. doi:10.1021/es9006433

Capone, D.G., Bautista, M.F., 1985. A groundwater source of nitrate in nearshore marine sediments. Nature 313, 214 216.

Cross, V.A., Bratton, J.F., Crusius, J., Kroeger, K.D., and Worley, C.R., 2012, Continuous resistivity profiling data from Northport Harbor and Manhasset Bay, Long Island, New York: U.S. Geological Survey Open-File Report 2011-1041, 1 CD-ROM.

Cross, V.A., Bratton, J.F., Kroeger, K.D., Crusius, J., and Worley, C.R., 2013, Continuous resistivity profiling data from Great South Bay, Long Island, New York: U.S. Geological Survey Open-File Report 2011-1040.

Flipse, W.J., Katz, B.G., Linder, J.B., Markel, R., 1984. Source of nitrate in ground water in sewered housing development, central Long island, New York. Ground Water 22, 418-426.

Hill, A.R., 1996. Nitrate removal in stream riparian zones. J. Environ. Qual. 25, 743–755.

Holocher, J., Peeters, F., Aeschbach-Hertig, W., Kinzelbach, W., Kipfer, R., 2003. Kinetic model of gas bubble dissolution in groundwater and its implications for the dissolved gas composition. Environ. Sci. Technol. 37, 1337–1343.

IPCC, 2013: Climate Change 2013: The Physical Science Basis. Contribution of Working Group I to the Fifth Assessment Report of the Intergovernmental Panel on Climate Change [Stocker, T.F., D. Qin, G.-K. Plattner, M. Tignor, S.K. Allen, J. Boschung, A. Nauels, Y. Xia, V. Bex and P.M. Midgley (eds.)]. Cambridge University Press, Cambridge, United Kingdom and New York, NY, USA, 1535 pp, doi:10.1017/CBO9781107415324.

Johannes, R.E., 1980. The ecological significance of the submarine discharge of groundwater. Mar. Ecol. Prog. Ser. 3, 365–373.

Kana, T.M., Darkangelo, O., Hunt, M.D., Oldham, B., Bennet, G.E., Cornwell, J.C., 1994. A membrane inlet mass spectrometer for rapid high precision determination of N_2, O_2, and Ar in environmental water samples. Anal. Chem. 66, 4166–4170.

Kana, T.N., Weiss, D.L., 2004. Comment on ‘‘Comparison of isotope pairing and N_2: Ar methods for measuring sediment denitrification’’ by B. D. Eyre, S. Rysgaard, T. Dalsgaard, and P. Bondo Christensen, 2002. Estuaries 25, 1077–1087. Estuaries, 2004 27, 173–176.

Korom, S.F., 1992. Natural denitrification in the saturated zone: a review. Water. Resour. Res. 28, 1657–68.

Kraft, B., Tegetmeyer, H. E., Sharma, R., Klotz, M. G., Ferdelman, T. G., Hettich, R. L., Geelhoed, J. S., Strous, M., 2014. The environmental controls that govern the end product of bacterial nitrate respiration. Science 345, 676−679.

Kroeger, K.D., Cole, M.L., Valiela, I., 2006. Groundwater-transported dissolved organic nitrogen exports from coastal watersheds. Limnol Oceanogr 51, 2248–2261.

Kroeger, K.D.; Swarzenski, P.W.; Greenwood, J.; Reich, C., 2007. Submarine groundwater discharge to Tampa Bay: Nutrient fluxes and biogeochemistry of the coastal aquifer. Mar. Chem. 391, 85-97.

Lee, Y.W., Hwang, D.W., Kim, G., Lee, W.C., Oh, H.T., 2009. Nutrient inputs from submarine groundwater discharge (SGD) in Masan Bay, an embayment surrounded by heavily industrialized cities, Korea. Science of the Total Environment 407, 3181-3188.

Lusczynski, N. J., Swarzenski, W. V., 1966. Salt-water encroachment in southern Nassau and southeastern Queens Counties, Long Island, New York. Geological Survey Water-Supply Paper 1613-F, 82 pp.Monti, J. Jr., Busciolano, R., 2009. Water-Table and Potentiometric-Surface Altitudes in the Upper Glacial, Magothy, and Lloyd Aquifers beneath Long Island, New York, March- April 2006: U.S. Geological Survey, Scientific Investigations Map 3066, 4 sheets.

NOAA, National Climatic Data Center, 2016. Annual Climatological Summary CSV. Website.

Monti, J. Jr., Scorsa, M..P., 2003. Trends in nitrogen concentration and nitrogen loads entering the South Shore Estuary Reserve from streams and ground-water discharge in Nassau and Suffolk counties, Long Island, New York, 1952-97, U.S. Geological Survey Publication, 2002-4255, 36pp.

NOAA, National Climatic Data Center, 2016. Annual Climatological Summary CSV; https://www.ncdc.noaa.gov/data-access/land-based-station-data.

Pabich, W.J., Valiela, I., Hemond, H.F., 2001. Relationship between DOC concentration and vadose zone thickness and depth below water table in groundwater of Cape Cod, U.S.A. Biogeochemistry **55,** 247–268.

Paerl, H.W., 1997. Coastal eutrophication and harmful algal blooms: Importance of atmospheric deposition and groundwater as "new" nitrogen and other nutrient sources. Limnol. Oceanogr. 42, 1154–1156.

Peterson, D.S., 1987. Ground-water- recharge rates in Nassau and Suffolk counties, New York: U.S. Geological Survey Water-Resources Investigations Report 86-4181.

Pluhowski, E.J., Kantrowitz, I.H., 1964. Hydrology of the Babylon-Islip area, Suffolk County, Long Island, New York: U.S. Geological Survey Water-Supply Paper 1768, 119 pp.

Rivett, M.O., Smith, J.W.N., Buss, S.R., Morgan, P., 2007. Nitrate occurrence and attenuation in the major aquifers of England and Wales. Q. J. Eng. Geol. Hydrogeol. 40, 335–352.

Rivett, M.O., Buss, S.R., Morgan, P., Smith, J.W.N., Bemment, C.D., 2008. Nitrate attenuation in groundwater: a review of biogeochemical controlling processes. Water Res. 42, 4215-4232. doi: 10.1016/j.watres.2008.07.020.

Schnoor, J.L., Licht, L.A., McCutcheon, S.C., Wolfe, N.L., Carriera, L.H., 1995. Phytoremediation: An Emerging Technology for Contaminated Soils. Environ. Sci. Technol., 29, 318-323A.

Seitzinger, S., Harrison, J.A., Böhlke, J.K., Bouwman, A.F., Lowrance, R., Peterson, B., Tobias, C., Van Drecht, G., 2006. Denitrification across landscapes and waterscapes: a synthesis. Ecol. Appl. 16, 2064–2090.

Smith, R. L., Böhlke J.K., Bongkeon, S., Tobias, C. R., 2015. Role of Anaerobic Ammonium Oxidation (Anammox) in Nitrogen Removal from a Freshwater Aquifer. Environ. Sci. Technol. 49, 12169−12177, DOI: 10.1021/acs.est.5b02488.

Steenhuis, T.S., Jackson, C.D., Kung, S.K.J., Brutsaert, W., 1985. Measurement of groundwater recharge on Eastern Long Island, New York, USA, J. Hydrol., 79, 145-169.

Stute, M., Forster, M., Frischkorn, H., Serejo, A., Clark, J.F., Schlosser, P., Broecker, W. S., Bonani, G., 1995. Cooling of tropical Brazil (5°C) during the Last Glacial Maximum, Science 269, 379–383.

Swarzenski, W. V., 1963. Hydrogeology of Northwestern Nassau and Northeastern Queens Gourdes Long Island, New York. Geological Survey Water-Supply Paper 1657 , 90 pp.U.S. EPA. 2010-2014 editions. Climate change indicators in the United States. https://www.epa.gov/climatechange/science/indicators/download.html.

Valiela I., Teal J.M., Volkman S., Shafer D. and Carpenter E.J. 1978. Nutrient and particulate fluxes in a salt marsh ecosystem: Tidal exchanges and inputs by precipitation and groundwater. Limnol. Oceanogr. 23, 798–812.

Vogel J.C., Talma, S.A., Heaton, T.H.E. 1981. Gaseous nitrogen as evidence for denitrification in groundwater. J.Hydrol., 50, 191-200.

Young, C., Kroeger, K.D., Hanson, G., 2013. Limited denitrification in glacial deposit aquifers having thick unsaturated zones (Long Island, USA). Hydrology J 21, 1773-1786.

Young, C., Tamborski, J., Bokuniewicz, H., 2015. Embayment scale assessment of submarine groundwater discharge nutrient loading and associated land use. Estuar Coast Shelf S. 158, 20-30.

Young, C., Martin, J.B., Hanson, G.H., 2016. Controls on Nitrous Oxide Production in, and Fluxes from a Coastal Aquifer in Long Island, NY, USA. J. Mar. Sci. Eng. 4, 71.

Weymann, D., Well, R., Flessa, H., von der Heide, C., Deurer. M., Meyer, K., Konrad, C., Walther, W., 2008. Groundwater N2O emission factors of nitrate-contaminated aquifers as derived from denitrification progress and N2O accumulation. Biogeosciences 5, 1215–1226.

Zhao, S., Zhang, P., Crusius, J., Kroeger, K., Bratton, J., 2011. Use of pharmaceuticals and pesticides to constrain nutrient sources in coastal groundwater of northwestern Long

Figure captions:

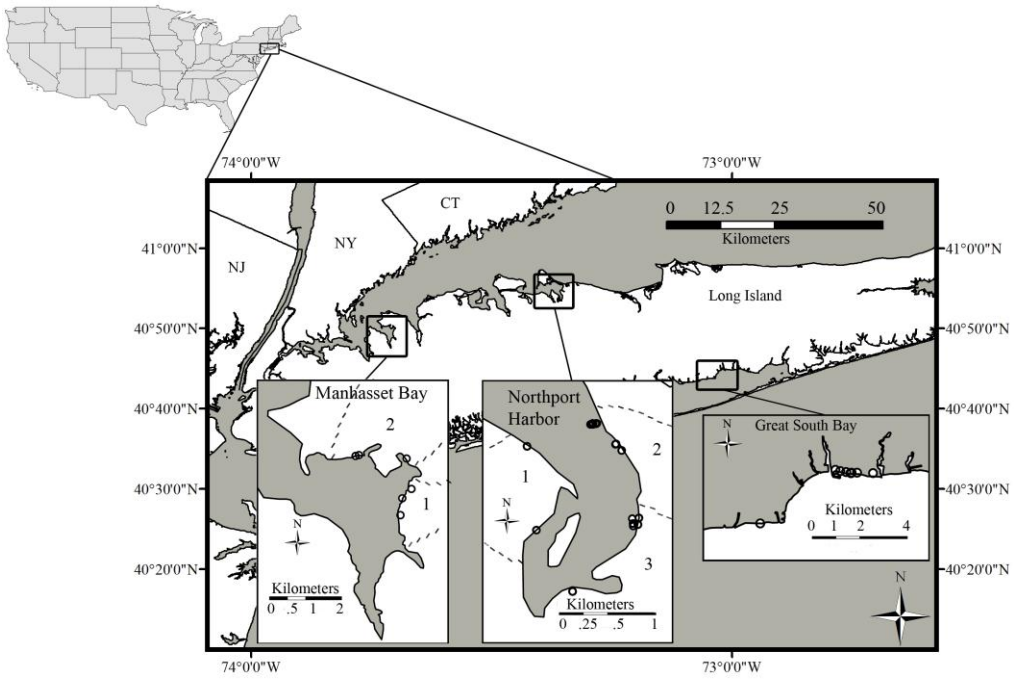

Figure 1. Map showing Long Island, NY, USA and study sites: Great South Bay, Manhasset Bay and Northport Harbor.

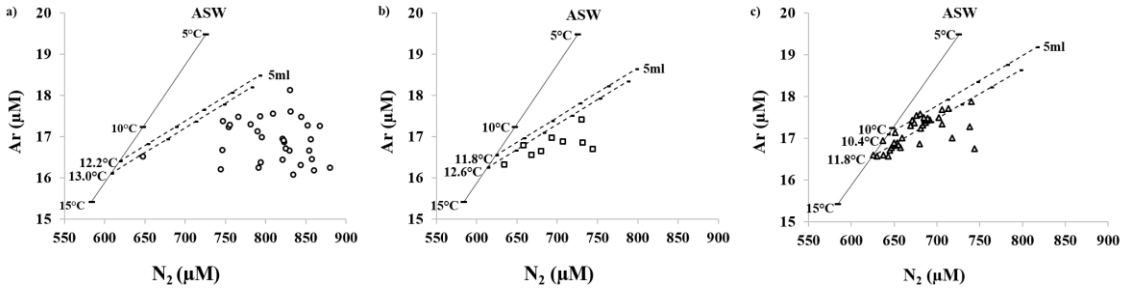

Figure 2. Concentrations of dissolved dinitrogen (N_2) and argon (Ar) in groundwater samples with salinity lower than 0.8 (S<0.8) collected from: a) Great South Bay (GSB), b) Manhasset Bay (MB), c) Northport Harbor (NH). The solid line represents the air-saturated water (ASW) curve at a range of recharge temperatures, while the dashed line shows expected increases in dissolved gas concentration from unfractionated excess air ranging in concentration from 0 to 5 mL of air per L of water, at the recharge temperatures indicated at the intersections of the ASW and excess air lines. Estimated recharge temperature ranged from a) 12.2˚C to 13.0˚C (GSB), b) 11.8˚C to 12.6˚C (MB), c) 10.4˚C to 11.8˚C (NH).

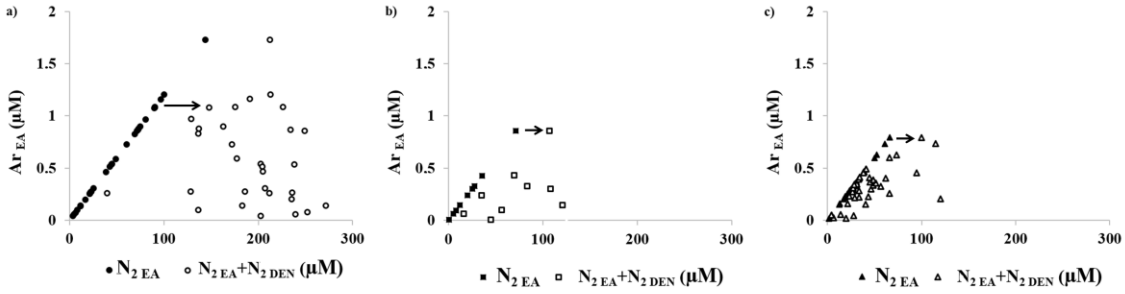

Figure 3. N_2 vs. Ar concentration in samples due to excess air (grey symbols), and N_2 vs. Ar concentration due to sum of excess air and denitrification (white symbols): a) Great South Bay (GSB), b) Manhasset Bay (MB), c) Northport Harbor (NH). Arrows represent direction of shift in N_2 concentration due to denitrification, and the distance along the x-axis for paired grey and white symbols for each sample represents magnitude of denitrification N_{2DEN}.

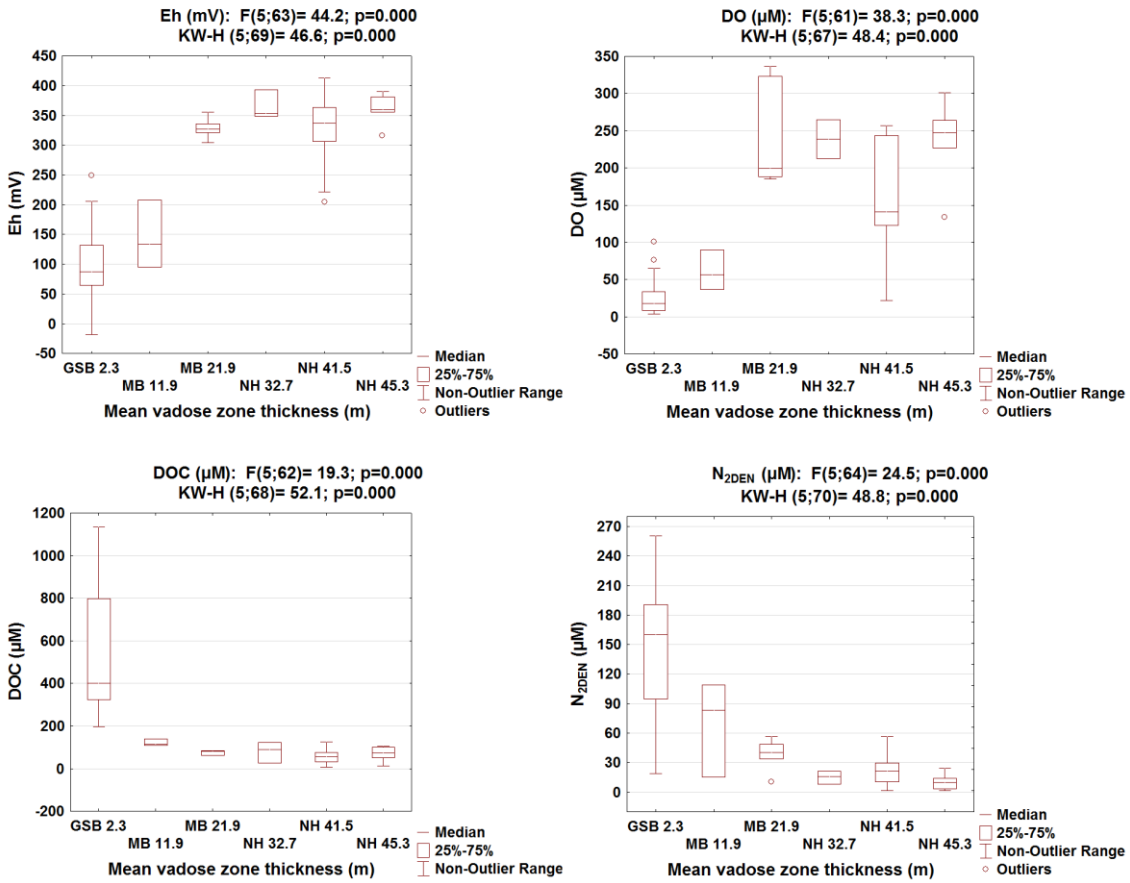

Figure 4. Box plots of oxidation-reduction potential (Eh), dissolved oxygen (DO), dissolved organic carbon (DOC), and denitrification (N_{2DEN}) versus mean vadose zone thickness (VZT) in watershed sections contributing groundwater to sampled shorelines of Great South Bay (GSB 2.3 m (n=32)), Manhasset Bay (MB 11.2 m (n=4) and 21.9 m (n=5)) and Northport Harbor (NH 32.7 m (n=3), NH 41.5 m (n=25) and NH 45.3 m (n=9)). Symbols F and KW-F indicate ANOVA and Kruskal–Wallis test, respectively.

Supporting Information

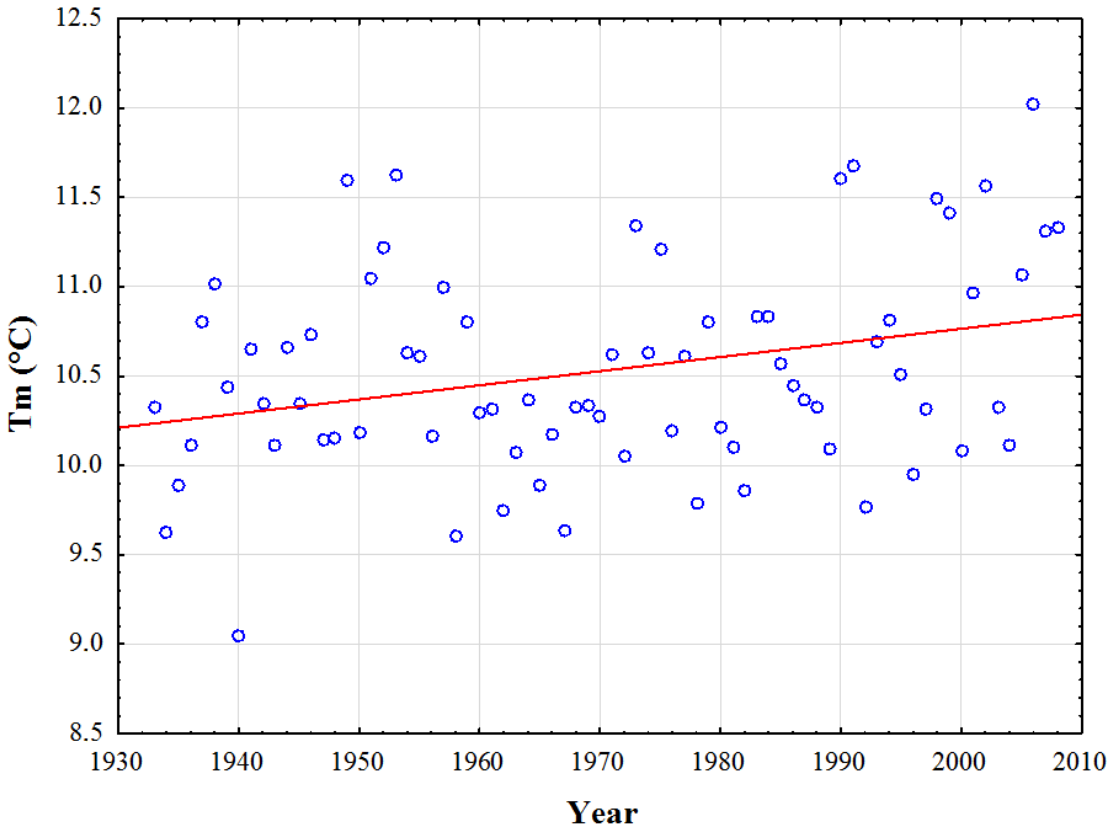

Figure S1. The mean annual air temperature (Tm) from 1930 to 2010 in Bridgehampton. Tm was calculated based on the monthly mean annual air temperatures (NOAA, 2016; https://www.ncdc.noaa.gov/data-access/land-based-station-data).

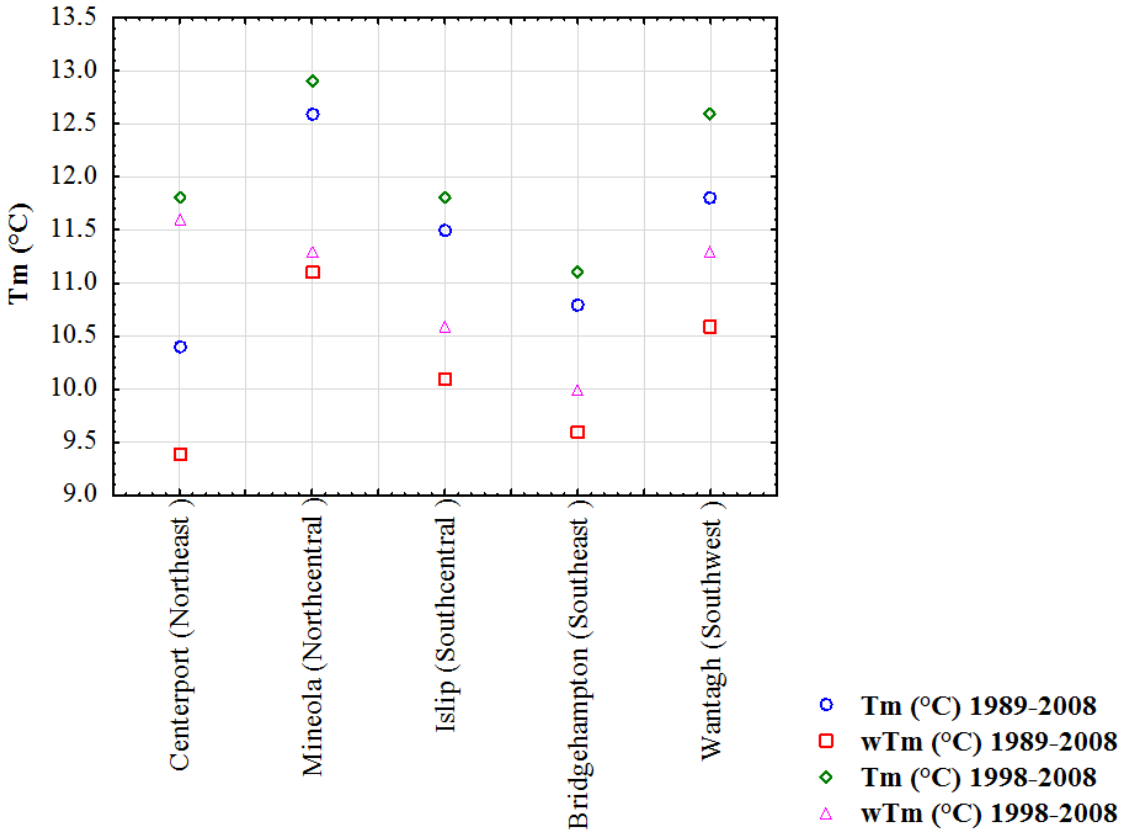

Figure S2. Mean annual air temperature (Tm) in several land-based stations located on Long Island, NY, USA (Centerport, Mineola, Islip, Bridgehampton, Wantagh). Tm was calculated based on the monthly mean annual air temperatures (NOAA, 2016; https://www.ncdc.noaa.gov/data-access/land-based-station-data). Weighted mean annual air temperature ($_{W}$Tm) were calculated based on 75% of recharge occurring in cooler part of the year, between October and May.

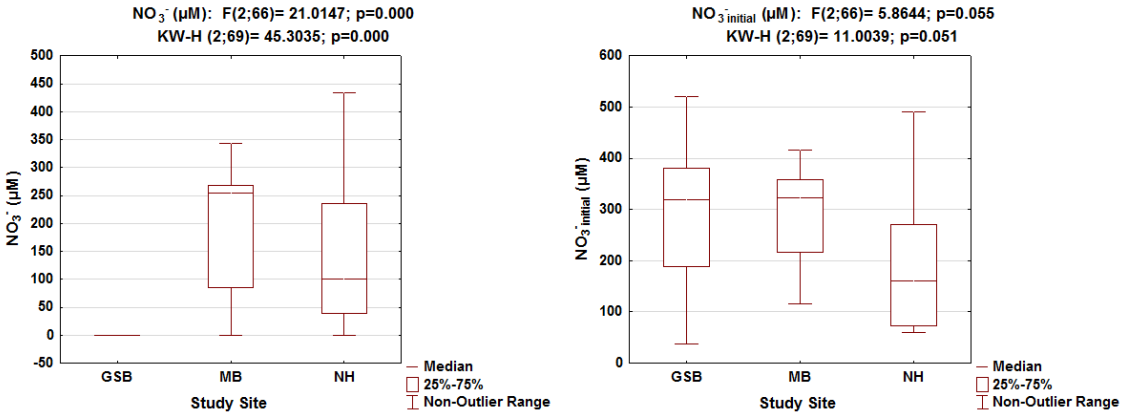

Figure S3. Box plots of NO_3^- and $NO_3^-{}_{initial}$ in Great South Bay (GSB, n=32), Manhasset Bay (MB, n=9) and Northport Harbor (NH, n=38). Symbols F and KW-F indicate ANOVA and Kruskal–Wallis test, respectively.

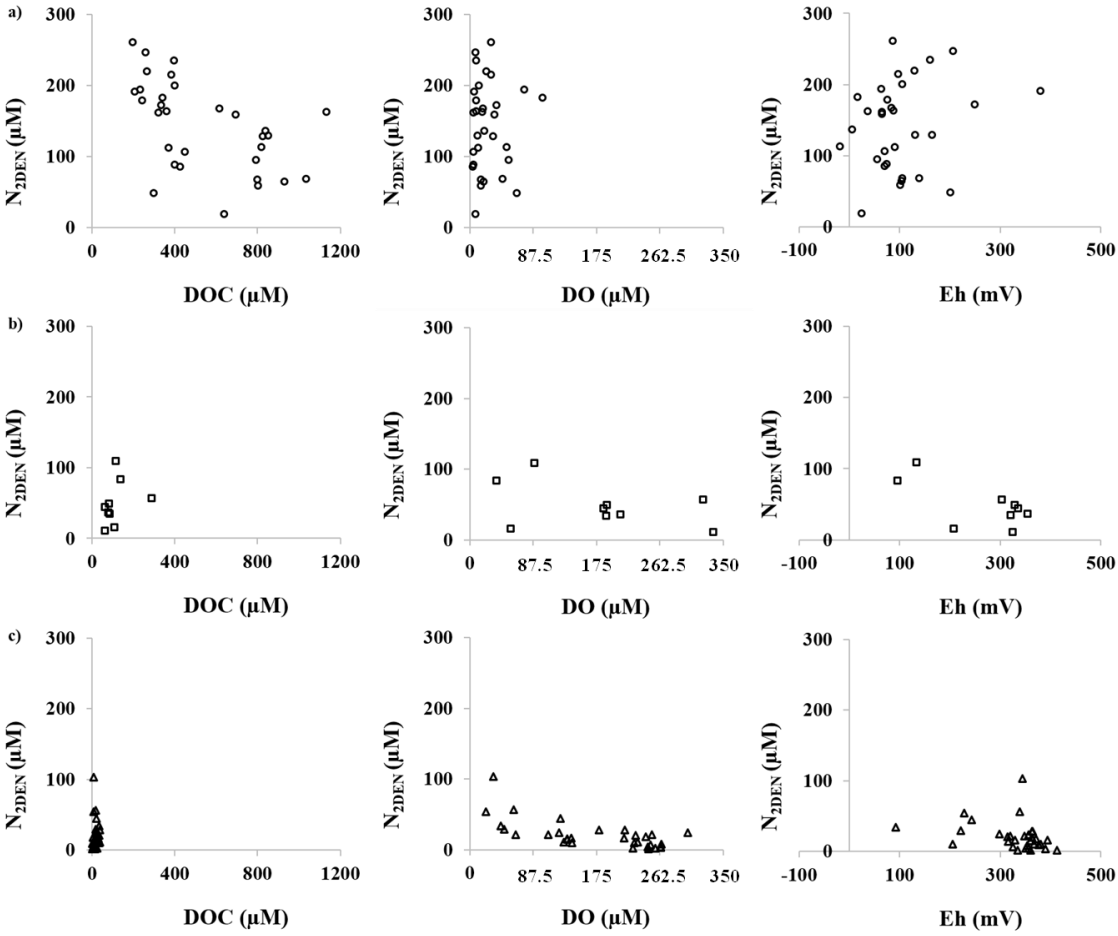

Figure S4. Relationships between nitrogen concentration coming from denitrification (N_{2D}) and dissolved organic carbon (DOC), dissolved oxygen (DO), and oxidation/reduction potential (Eh) at a) Great South Bay (GSB), b) Manhasset Bay (MB) and c) Northport Harbor (NH).

Table S1-Sn. Tritium/He measurements (Noble Gas Laboratory Lamont-Doherty Earth Observatory of Columbia University, New York).

Sample ID	Site	Age	
		Uncorrected Age±1σ (y)	Corrected for terrigenic He Age±1σ (y)
pic4	Great South Bay	7.2±0.6	8.0±0.5
MIZ5	Manhasset Bay	10.3± 0.5	12.2±0.5
MIZ6	Manhasset Bay	12.3±0.5	15.0±0.6
MIZ7	Manhasset Bay	5.1±0.3	7.9±0.3
niy6	Northport Harbor	-10.5±1.2	-6.9±0.5
niy7	Northport Harbor	-2.2±0.4	0.4±0.0
niy8	Northport Harbor	-2.8±0.4	0.9±0.1

Table S2-Sn Groundwater data for samples collected in Great South Bay, Manhasset Bay and Northport Harbor during spring and fall 2008.

Location	Sample ID	Depth (m)	Salinity	pH	Eh (mV)	DO (µM)	DOC (µM)	NO_3^- (µM)	NH_4^+ (µM)	Ar (µM)	N_2 (µM)	N_{2DEN} (µM)
Great South Bay (GSB)	A1	1.7	0.1	5.8	249.2	37.5	335.4	20.5	27.0	16.2	791.5	171.9
	mascot 1	2.0	0.3	6.9	6.4	20.0	838.5	0.1	252.9	17.5	844.4	136.1
	pd1	2.2	0.5	6.6	24.5	8.5	638.9	0.1	919.8	16.5	648.1	18.7
	pd14	2.7	0.6	7.0	37.5	17.5	1134.4	0.1	268.0	17.3	852.4	162.0
	pd17	1.4	0.5	6.6	88.0	9.1	360.0	0.0	538.0	16.4	793.9	163.4
	pd2	0.5	0.3	6.5	164.9	32.5	826.4	0.0	247.6	16.2	744.6	128.5
	pd4	0.9	0.4	6.4	201.0	65.7	297.5	43.7	35.0	17.4	747.3	48.6
	pd9	2.0	0.7	6.8	139.5	45.3	1034.9	0.0	36.7	18.1	830.6	68.4
	PIA-10	7.3	0.4	6.5	129.8	24.0	267.2	0.0	282.8	16.3	843.7	219.2
	PIA-6	3.3	0.6	6.8	-18.5	51.0	819.1	0.0	159.2	17.6	831.1	112.7
	PIA-7	4.3	0.7	6.6	55.4	54.4	794.7	0.0	209.7	17.6	809.2	94.4
	PIA-8	5.3	0.4	6.8	97.0	29.4	385.3	0.0	126.2	16.7	854.3	214.2
	PIA-9	6.3	0.4	6.8	77.8	25.7	345.1	0.0	139.3	16.1	834.7	-
	PIB-4	1.3	0.6	6.7	104.1	19.4	931.4	0.0	212.9	17.3	755.5	64.3
	PIB-5	1.8	0.5	6.8	131.4	11.3	851.2	0.0	230.0	17.0	795.8	128.7
	PIB-6	2.8	0.7	6.8	100.9	16.0	802.0	ND	ND	17.5	766.3	58.4
	PIB-7	3.8	0.4	6.7	106.2	13.2	400.9	0.1	161.0	16.4	821.2	199.8
	PIB-8	4.8	0.6	6.5	90.4	11.6	372.5	0.1	266.6	17.1	790.4	111.8
	PIC-2	0.5	0.5	7.0	105.0	15.3	798.7	0.0	258.9	17.2	754.7	67.7
	PIC-3	1.0	0.4	7.1	84.5	18.5	617.3	0.1	237.9	16.9	823.3	166.6
	PIC-4	2.0	0.7	7.2	65.4	34.1	696.0	0.0	229.0	16.9	821.2	158.2
	PIC-5	4.0	0.4	7.0	74.0	5.0	401.9	0.1	185.6	17.3	781.3	88.4
	PIC-6	5.0	0.4	6.7	161.0	8.7	397.1	0.1	297.3	16.5	857.5	234.8
	PIC-7	6.0	0.4	6.6	206.0	7.9	259.5	0.0	471.4	16.2	860.5	246.4
	PIC-8	7.0	0.6	6.3	381.0	6.0	205.9	0.0	277.3	16.7	830.0	190.6
	PID-2	0.5	0.4	6.9	71.0	4.9	449.9	0.0	392.7	16.7	746.7	105.8
	PID-3	2.0	0.4	6.9	71.0	4.0	427.1	0.1	391.7	17.5	793.6	85.1
	PID-4	3.0	0.3	7.0	65.0	5.0	323.5	0.0	441.1	16.9	822.4	161.7
	PID-5	4.0	0.4	6.8	76.0	8.9	244.3	0.0	331.6	17.3	867.7	178.2
	pie3	2.0	0.4	6.9	16.0	101.0	340.6	0.0	510.6	16.7	825.5	181.9
	pie4	4.0	0.4	6.7	63.7	76.0	232.7	0.0	355.6	16.9	856.3	193.8
	pie5	5.0	0.4	6.5	86.5	30.0	196.9	0.0	593.2	16.2	879.9	260.6
Manhasset Bay (MB)	MD5	2.4	0.3	6.5	325.0	336.6	62.9	337.1	0.0	16.3	634.3	11.0
	MD6	3.7	0.6	7.3	303.8	323.2	288.2	267.9	0.0	16.9	707.1	56.5
	MD7	2.4	0.2	6.8	134.2	90.0	114.3	0.0	5.0	16.7	744.2	108.7
	MD8	2.4	0.3	6.8	95.7	36.9	138.8	0.3	43.1	16.8	731.7	83.3

	MD9	2.4	0.2	7.0	207.7	56.6	110.3	85.6	1.1	16.8	658.6	15.4
	MIA4	3.9	0.5	6.3	355.3	208.8	78.8	343.4	0.0	17.4	730.7	35.9
	MIA5	4.4	0.5	6.5	320.5	188.8	85.2	253.8	0.0	17.0	693.1	34.1
	MIA6	4.9	0.8	6.3	329.5	190.0	82.6	154.6	0.0	16.6	679.9	48.6
	MIB7	7.0	0.2	6.4	335.9	185.3	62.7	266.4	0.0	16.6	668.1	44.3
Northport harbor (NH)	**ND11**	2.4	0.1	6.0	355.7	301.3	12.6	24.7	0.0	17.1	651.1	24.1
	ND16	1.2	0.3	6.6	384.3	321.3	145.1	243.2	0.5	16.6	625.6	-
	ND19	3.0	0.7	6.4	393.3	212.8	27.1	293.4	0.1	17.7	706.1	16.1
	NI10	5.2	0.5	6.3	366.0	249.4	36.6	79.3	0.0	17.5	676.0	-
	NI11	5.9	0.6	6.3	359.4	249.1	41.5	102.1	0.0	17.5	337.3	-
	NI12	6.9	0.6	6.2	380.8	232.2	56.8	89.9	0.6	17.3	669.0	10.7
	NI13	7.8	0.6	6.8	366.3	226.9	51.2	ND	0.0	17.4	673.8	10.0
	NI2	0.5	0.8	6.2	316.2	134.1	72.3	48.7	0.0	17.5	685.1	14.2
	NI4	2.0	0.4	6.2	348.3	63.5	123.6	65.2	0.0	17.4	686.4	21.4
	NIC10	7.6	0.1	6.1	353.2	265.0	90.2	204.6	0.0	16.7	644.9	8.4
	NIC11	8.0	0.2	6.3	336.6	257.5	90.2	200.5	0.0	16.9	649.7	-
	NIC12	8.5	0.1	6.1	350.4	246.3	111.3	204.7	0.0	16.6	629.7	4.5
	NIC14	9.5	0.1	6.0	359.8	247.2	73.8	196.3	0.0	16.9	650.2	1.3
	NIC8	6.6	0.1	6.1	356.3	264.1	106.1	140.5	0.0	16.8	646.7	4.3
	NIC9	7.1	0.1	6.1	389.7	264.1	100.5	219.6	0.0	16.8	649.6	3.4
	NIE11	8.5	0.8	5.8	313.9	251.1	77.2	233.9	0.0	17.7	713.5	21.1
	NIE12	8.9	0.3	5.9	324.8	249.7	62.4	249.6	0.0	16.8	654.5	6.8
	NIF2	1.0	0.7	7.3	91.6	42.8	91.9	0.6	8.0	17.9	740.1	33.8
	NIF3	2.0	0.1	6.8	221.8	47.2	126.6	0.4	19.1	16.9	679.7	29.4
	NIF4	3.0	0.1	6.5	311.8	159.4	71.7	63.2	0.7	16.9	636.7	-
	nis1	0.5	0.1	7.1	320.2	108.2	ND	23.3	0.4	17.4	691.4	21.4
	nit1	0.5	0.8	7.4	297.6	123.2	48.2	23.6	0.3	17.3	683.6	24.5
	nit2	1.0	0.2	6.8	329.0	140.0	35.2	41.3	0.3	17.5	688.8	16.2
	nit3	1.5	0.5	7.3	204.6	129.7	ND	39.7	0.5	17.5	684.8	10.8
	nit5	2.5	0.3	6.5	334.8	225.0	31.7	57.2	2.5	17.4	671.2	2.2
	niw2	1.0	0.8	6.1	362.7	178.5	49.5	109.9	0.3	17.2	680.8	28.1
	niw3	1.5	0.5	6.4	343.8	32.5	61.4	7.8	0.4	16.7	743.6	103.3
	niw4	2.0	0.5	6.5	338.4	60.3	77.0	43.4	0.1	17.0	717.7	56.5
	niy8	9.5	0.1	6.2	371.2	243.2	59.7	235.2	0.2	16.6	642.8	18.0
	ND10	1.1	0.3	6.9	311.0	213.5	5.7	134.3	0.0	17.6	680.6	-
	ND12	1.1	0.5	7.1	243.2	125.0	16.1	65.3	6.8	17.3	705.9	44.4
	ND13	1.1	0.2	5.7	416.6	102.8	78.5	312.8	0.0	17.0	659.0	-
	ND14	0.3	0.2	6.1	412.7	256.6	59.8	316.9	0.8	16.9	653.4	1.8
	ND21	1.2	0.3	5.8	376.6	141.0	57.6	389.6	0.0	16.6	637.5	9.8

	ND22	1.8	0.3	5.9	360.5	134.7	53.0	412.2	0.0	16.8	657.0	15.1
	ND23	0.3	0.2	6.2	364.1	214.4	28.5	434.5	0.0	17.5	701.9	28.2
	ND33	2.1	0.1	6.4	363.3	228.8	18.2	272.7	0.0	17.4	688.4	20.2
	ND8	0.9	0.1	6.5	227.7	22.2	8.4	1.0	0.9	17.3	738.4	54.0